Global Advanced Research Journal of Chemistry and Materials Science Vol. 1(3) pp. 055-062, September, 2012
Available online http://garj.org/garjcms/index.htm

Full Length Research Paper

Effects of heat treatment on the electrochemical corrosion behaviour of aluminum alloy AA3003 in an aqueous acid media

Okeoma Kelechukwu B[1], Owate Israel O[2]*, Oguzie Emeka E[3], Mejeha Ihebrodike M[1].

[1]Materials Science Group, Department of Physics, Federal University of Technology, Owerri, Nigeria.
[2]Materials Science Group, Department of Physics, University of Port Harcourt, Nigeria.
[3]Electrochemistry and Materials Science Research Unit, Department of Chemistry, Federal University of Technology, Owerri, Nigeria.

Accepted 18 August, 2012

The effect of heat treatment and quenching regimen on the electrochemical corrosion behaviour of aluminium alloy AA3003 in 0.1M H_2SO_4 was studied by open circuit potential, potentiodynamic polarization and electrochemical impedance spectroscopy measurements. Three different specimens (untreated, air-quenched and oven-quenched) were investigated. Polarization results show that all the specimens underwent active dissolution, with no distinctive transition to passivation, although heat treatment was observed to shift the corrosion potential towards more cathodic values and increased the rates of the cathodic and anodic partial reactions of the corrosion process. The impedance spectra for all the specimens comprised a high frequency capacitive loop and an inductive loop at low frequency and reveal lower values of the charge transfer resistance for the heat treated specimens. All of the results indicate that heat treatment diminished the corrosion resistance of AA3003 in 0.1M H_2SO_4, without modifying the mechanism of corrosion. The corrosion resistance decreased in the order; untreated > air-quenched > oven-quenched. This trend has been correlated with the phase constituents of the different specimens as determined from x-ray diffraction (XRD) and scanning electron microscopy (SEM).

Keywords: AA3003, heat treatment, quenching, acid corrosion, electrochemical measurements.

INTRODUCTION

Aluminium and its alloys have excellent physical and chemical properties and presently find extensive industrial as well as domestic applications (Abdel-Gaber et al., 2008; Emreguil and AbbasAksilt, 2000; Stefano et al., 2008; Fellener et al., 1981; Yang, 1994; Balaji and Radhakrishnan, 2006; Komisarov et al., 1996; Diaz-Ballote et al., 2009; Nobe et al., 1999; Guillaumin and Mankowski, 1999; Dymek and Dollar, 2003; Rosliza et al., 2008). As a result of this, investigation of the corrosion behaviour in different aggressive environments has continued to generate considerable attention. The materials exhibit corrosion resistance in many environments due essentially to the initial formation of a compact and adherent passive oxide film on the exposed surfaces. This oxide film is stable over the pH range 4 to 9, which is why the materials have remarkable corrosion resistance to most natural environments. However, the

*Corresponding Author E-mail: owateio@yahoo.com

oxide film is amphoteric and hence dissolves readily in strong acidic and alkaline media, initiating metal dissolution (Vargel, 2004)

Al-Mn alloys are often used in heat exchanger systems, where they undergo series of heating and cooling sequences in a variety of aggressive environments, which undoubtedly affect the strength and stability of the alloys. In the course of the exposure to high temperatures, second phases are often formed, which are either cathodic or anodic relative to the metal matrix, depending on the nature of the environments. The difference in potential between the second phases and the metal matrix could normally give rise to galvanic cell formation (Sinyavskii, 2001; Buchheit et al., 1994), which, depending on the nature of interaction with the environment, could either accelerate or hinder the corrosion rate. Accordingly, the present study investigates the impacts of heat treatment on the electrochemical corrosion behaviour of aluminum alloy AA3003 in 0.1M H_2SO_4. Attempts have also been made to assess the phase constituents of the different specimens by x-ray diffraction (XRD) and scanning electron microscopy (SEM).

EXPERIMENTAL

MATERIALS PREPARATION

Aluminium alloy AA3003 used in this study was obtained from First Aluminum PLC Port Harcourt, Nigeria and had the following weight-percentage composition (Si = 0.36; Fe = 0.55; Cu = 0.077; Mn = -1.22; Mg = 0.055; Zn = 0.0042; Ti = 0.026; Cr = 0.0068; Ni = 0.0015; V = 0.0087; Pb = 0.064; Al = balance) The heat treated specimens were subjected to a temperature of 150^0 C in a furnace for 1 h, and subsequently divided into two sets; one set was removed from the furnace and allowed to cool in open air, while the other set was left in the furnace to cool at a rate of $0.2^oC/h$ in order to mimic the gradual cooling sequence found in heat exchanger chambers.

The untreated, air-quenched and oven-quenched samples were all machined into coupons of dimensions 1.5 cm x 1.5 cm, which were wet-polished with silicon carbide abrasive paper (from grade #200 to #1000), degreased in acetone, rinsed with distilled water and dried in warm air. These were subsequently sealed with epoxy resin in such a way that only one square surface of area 1.0 cm^2 was left uncovered.

Materials characterization

Structural characteristics of the as received AA3003 and heat treated and quenched specimens were analyzed by X-ray diffraction (XRD, XPERT-PRO) using Cu Kα radiation as well as by scanning electron microscopy (SEM, Shimadzu SSX-550). XRD measurements were undertaken to enable verification of the phase constitution before and after heat treatment/quenching. SEM imaging was used to identify surface defects (including inhomogeneities and porous intensity) arising from the different heat treatment/quenching regimen.

Electrochemical measurements

Electrochemical experiments were conducted in a conventional three-electrode cell using a VERSASTAT 400 Complete DC Voltammetry and Corrosion System, with V3 Studio software. A platinum foil was used as counter electrode and a saturated calomel electrode (SCE) as reference electrode. The later was connected via a Luggin's capillary. The test electrolyte was 0.1 M H_2SO_4, prepared from analytical reagent grade concentrated acid using distilled water. Measurements were performed in aerated and unstirred solutions at the end of 1 h of immersion at 30^oC. Impedance measurements were made at corrosion potentials (E_{corr}) over a frequency range of 100 kHz – 10 mHz, with a signal amplitude perturbation of 5 mV. Potentiodynamic polarization studies were carried out in the potential range -1.1 to 1.0 V versus the corrosion potential at a scan rate of $1mVs^{-1}$. Each test was run in triplicate to verify the reproducibility of the systems.

RESULTS AND DISCUSSION

Structural analysis

XRD spectra

Figure 1 shows the XRD patterns of the untreated, air quenched and oven quenched samples of AA3003. It is easily seen that all three samples display distinct, sharp, and narrow peaks, due to the crystalline nature of the AA3003 alloy. The crystallite size was determined using Debye- Scherrer's formula as follows (Cullity, 1978);

$$D = \frac{0.9\lambda}{\beta \cos\theta} \qquad (1)$$

D is the crystallite size, λ is the incident radiation wave length, β is the full width at half maximum of the profiles and θ is the angular position.

The untreated sample can be seen to possess fewer but more intense peaks compared to the heat treated samples, which mean that heat treatment lowered the degree of crystallinity of the alloy (Ruhi et al., 2009). Again, the heat treated samples show multiple of peaks with lower intensity, suggesting that heat treatment promoted splitting or growth of additional crystallites. Li and Arnberg (Li and Arnberg, 2003) observed that the break up, growth and coarsening mechanisms in heat treated DC cast aluminium alloy AA3003 contribute to the size, and area fraction of the intermetallic particles.

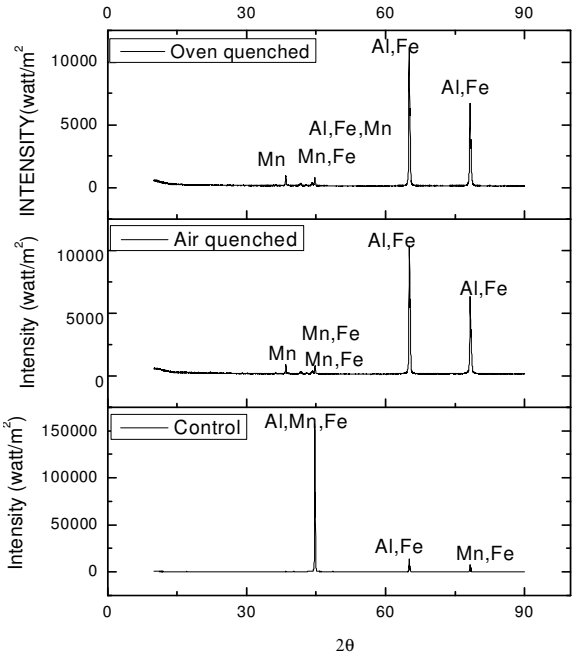

Figure 1. XRD Spectra of control, oven quench and air quench sample

Accordingly, the AlMnFe crystalline phase with peak intensity 153,858 wm^{-2} (17.95 Å) found in the untreated sample, is completely absent in the air-quenched sample, but appears at very low intensity (673.79 wm^{-2}; 14. 59 Å) in the oven-quenched sample. The crystallites AlFe phase and MnFe phase are present in all the samples, but the peak intensity of AlFe is slightly lower in the heat treated samples, while MnFe is slightly minimized and appears at lower diffracting angles in the heat treated samples. It is also evident that heat treatment induced multiplicity of the AlFe crystallite, which may include the Al_3Fe phase, which is nobler than the Al matrix and could thus induce anodic dissolution of the Al matrix (Buchheit, 1995; Szklarska- Smialowska, 1999). Notable also is the precipitation of Mn crystallites in the heat treated samples.

Furthermore, Li and co-worker (Li and Arnberg, 2003) observed that precipitation of Mn onto the particles from supersaturated matrix influence the size and composition of the primary particles. Enrichment of Mn in the second phase particles forms galvanic cell effects relative to the adjacent Al alloy substrate, which modify the electrochemical properties of the substrate (Liu and Cheng, 2010). Figure 1 also reveals close similarities in the composition of intermetallic particles in the two heat treated samples, but their sizes are slightly smaller in the air-quenched specimen. This possibly suggests that the oven quenching procedure modified the microstructure of the AA 3003 alloy to a greater extent. Again, the AlFeMn phase (identified as Al_6FeMn (Abdel-Gaber et al., 2008)) which is present in the oven-quenched sample did not appear in the XRD pattern of the air-quenched specimen. These two observations illustrate the effect of the different quenching procedures on the structural characteristics of heat treated AA 3003 alloy.

SEM morphological images

SEM micrographs of the untreated, air-quenched and oven quenched specimens are illustrated in Figure 2. The untreated specimen (Figure 2a) presents clear evidence of large coarse white grain phases, as well as cloudy grey and dark grey phases which gave the different peaks in the XRD of Figure 1. For the air-quenched sample (Figure 2b), there are smaller grain phases which consist of tiny white phases, cloudy grey phases, and dark cloudy phases, all of which cover the entire surface of the sample. The oven-quenched sample shows linear patterns of distinct dark and grey phases, with tiny white patches distributed sparingly on the sample. From the SEM micrographs it clear that heat treatment caused the intermetallic grain particles to dissolve to tiny particles, in agreement with the XRD results.

Electrochemical measurements

Open circuit potential measurements

The variation of the open-circuit potential (E_{ocp}) with time

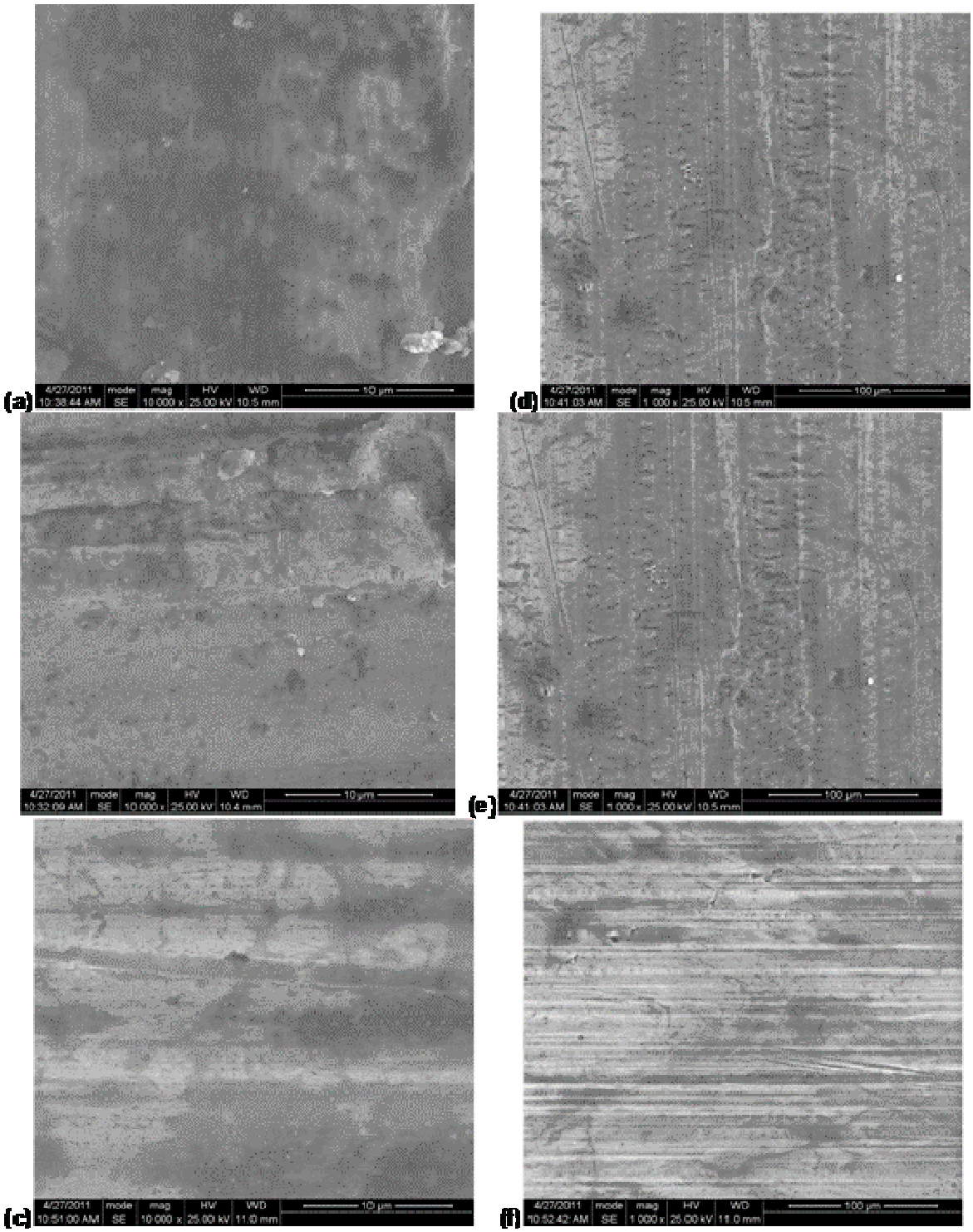

Figure 2: The SEM images of control (a & d), air quenched (b & e), and (c and f) oven quenched sample of AA3003, (a, b, c, =5000x; d, e, f =500x).

for all AA3003 specimens in 0.1 M H_2SO_4 solution is shown in Figure 3. A steady decrease in E_{ocp} is observed for all systems due to the dissolution of the air-formed oxide films on the electrode surfaces. Although there are no pronounced differences in the values of E_{ocp} for the three specimens, it is obvious that heat treatment shifts the E_{ocp} of AA3003 towards more positive (noble) potentials. This effect, could be attributed to the

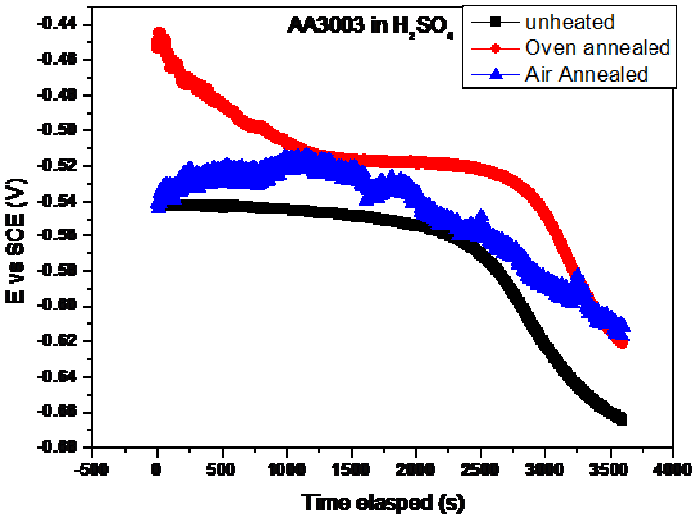

Figure 3. The open circuit Eocp for control, oven and air quenched samples in sulphuric acid environment.

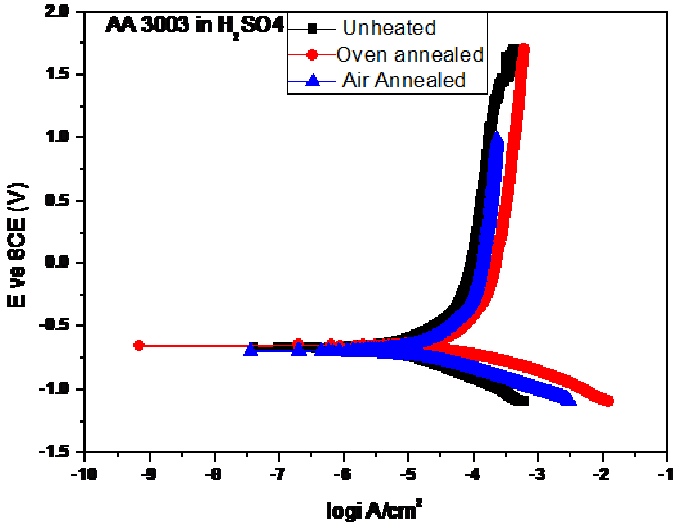

Figure 4. The Potentiodynamic profile of control, oven and air quenched samples of AA3003 aluminium alloy in sulphuric acid environment.

dissolution of the precipitated intermetallic particles on the alloy surface on heating, and is more pronounced for the oven-quenched sample.

For instance, Al_3Fe that precipitates on the oven-quenched specimen is nobler than the Al matrix and thus reduces the number of active dissolution sites on the alloy surface (Birbilis and Buchheit, 2005).

Potentiodynamic polarization measurements

Typical potentiodynamic polarization curves for the untreated, oven-quenched and air-quenched samples of AA3003 in 0.1 M H_2SO_4 are presented in Figure 4. The corresponding electrochemical parameters are given shown in table 1. All three samples exhibit active dissolution with no distinctive transition to passivation up to about 1.0 V versus SCE. The similarity of the polarization curves for the three specimens suggests comparable corrosion mechanisms. It is, however obvious that heat treatment has a negative influence on the polarization behaviour of AA3003 in 0.1 M H_2SO_4, increasing both the anodic and cathodic current densities and shifting in the cathodic direction, corresponding to a decrease in the polarization resistance and/or an increase in the corrosion current density (Table 1). The

Table 1. Polarization resistance (R_p) and corrosion current density ($I_{Corr.}$) for untreated, oven-quenched and air- quenched samples of AA3003 in 0.1MH_2SO_4

Sample	R_p (Ωcm^{-2})	Icorr (μAcm^{-2})
Un heated or Control	5822.8	3.714
Oven quenched	2685.4	8.095
Air quenched	4110.6	5.289

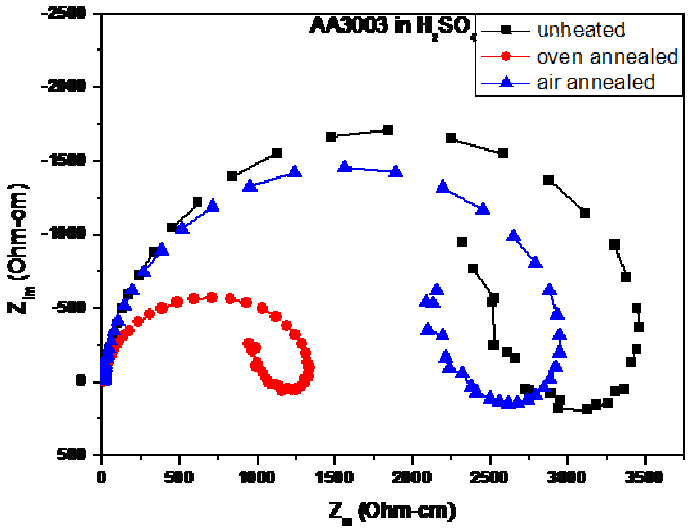

Figure 5. Electrochemical Impedance Spectroscopy of Control, Oven and Air quenched Samples of AA3003 aluminum alloy in sulphuric acid environments.

deleterious consequence of heat treatment, which could be attributed to the higher corrosion susceptibility of the intermetallic particles precipitated on the alloy surface on heating, was more pronounced on the oven-quenched specimen.

Impedance measurements

Electrochemical impedance spectra were measured at the open circuit potential for the different AA3003 specimens in 0.1 M H_2SO_4 solution. The obtained impedance responses are presented in Nyquist and Bode formats in Figure 4. All the specimens display similar impedance features; each Nyquist plot is characterized by a single depressed capacitive semicircle from high to intermediate frequencies followed by a low frequency inductive arc. The phase angle vs. frequency plots comprise a peak at high to intermediate frequencies and a valley at low frequencies, which respectively represent the capacitive and inductive characters, which have been reported for aluminium dissolution in various media (Abdel-Gaber et al., 2008, Sherif and Su-Moon, 2006; Santos et al., 2003). According to Santos et al. (Santos et al., 2003), these features result from interactions between dissolution of the more active phases in the alloy and charge transfer processes within the double layer, related to the Al rich phase attack. The capacitive loop can be attributed to charge transfer processes associated with the effect of the double layer capacitance and its diameter is related to the charge transfer resistance (R_{ct}) at the metal/solution interface, while the inductive loop probably results from the adsorbed intermediate products (Ambat et al., 2006; Park et al., 1999).

The Nyquist plots clearly show that heat treatment decreased the diameter of the capacitive arc, hence R_{ct} which corresponds to a reduction in the corrosion resistance of AA3003 in 0.1 M H_2SO_4. This effect is more pronounced for the oven-quenched sample and points towards the high corrosion susceptibilities of the heat treated samples in the sulphuric acid medium. R_{ct} decreased in the order untreated > air-quenched > oven-quenched, which is in agreement with the trend of corrosion resistance predicted by the polarization data.

The corrosion behaviour of the heat treated samples can be related to the features of the intermetallic particles arising from the heat treatment as illustrated in the XRD spectra (Figure 5). The corrosion behaviour of the heat

Table 2. Impedance parameters for the untreated, air-quenched and oven-quenched AA3003 in 0.1 M sulphuric acid environment

Parameter	Control/Unheated	Oven quenched	Air quenched
Resistance $R_s(\Omega cm^{-2})$	21.13	8.607	8.525
Constant Phase Element CPE Y x 10^{-5}	1.115	1.883	1.066
Frequency n	0.9355	0.9139	0.9276
Resistance $R_1(\Omega cm^{-2})$	3656	1330	2758
Inductance L (mH)	7173	4447	4458
Resistance R_2 (Ωcm^{-2})	1.153x 10^4	5774	6700

treated samples can be better explained by the fact that the comparatively finer particle phases resulting from the heat treatment and quenching provide high population of corrosion sites, as well as large volume of grain boundaries, which promote both corrodent attack as well as corrodent transport within the alloy surface.

To obtain the numerical values of the various impedance parameters presented in Table 2, the impedance spectra were analysed by fitting to the equivalent circuit model $R_s(QR_1(LR_2))$, R_s is the solution resistance which is the uncompensated resistance between the working electrode and the reference electrode, R_1, is the leakage resistance associated with the constant phase element Q, that is used to model deviation from an ideal capacitor, R_2 is the resistance offer to the migrating ions in the solution that manifested in the magnetic fields with its associated inductance L which existed at certain frequency range for a particular sample,(Okeoma et al., 2011).

The constant phase element Q decreased for heat treated specimens, and more so for the air-quenched specimen. The CPE is used in place of a capacitor to compensate for deviations from ideal dielectric behaviour arising from the inhomogeneous nature of the electrode surfaces. The impedance of the CPE is given by $Z_{CPE} = Q^{-1} (j\omega)^{-n}$, where Q and n represent the magnitude and exponent of the CPE respectively, j is an imaginary number and ω is the angular frequency in rad s^{-1}. Lower Q_{dl} values corresponds to reduced interfacial capacitance, which, according to the Helmholtz model ($C_{dl} = \varepsilon\varepsilon_o A/\delta$); results from a decrease in the dielectric constant (ε) or an increase in the double layer thickness (δ). ε is the dielectric constant of the medium, ε_o the vacuum permittivity, A the electrode area and δ the thickness of the interfacial layer. The observed reduction in Q_{dl} values of heat treated samples would most likely result from an increase in the thickness of the double layer, since the dielectric constant of the medium is not expected to vary significantly. Moreover, the precipitation of intermetallic particles on heat treatment is expected to lead to an increase in the thickness of the double layer; the pertinent issue however is whether the resulting surface film is compact and protective, or porous and non -protective. To this end, the high corrosion susceptibility of the heat treated samples clearly imply that the surface films are non -protective and interestingly, the trend of Q_{dl}, hence double layer thickness (untreated < oven-quenched< air-quenched) correspond exactly with the trend of corrosion resistance.

CONCLUSION

Electrochemical investigation of heat treated aluminium alloy AA3003 carried out to study the effects of oven and air quenching on the electrochemical properties of the alloy system. In order to give credence to the observed changes in the electrochemical properties, XRD and SEM investigations were undertaken. It can therefore be concluded that:

- The heat treatment caused the splitting of the spectra peaks, but decrease in intensity as observed in the XRD and SEM diagrams.
- The open circuit potentials of the heat treated samples shifted to the higher potentials. This may be attributed to the dissolutions of the precipitated intermetallic particles such as Al_3Fe, which is nobler than the matrix.
- The potentiodynamic polarization measurements reveal that the heat treatment caused both anodic and cathodic dissolutions of the alloy. This results in the increase in both anodic and cathodic current densities.
- The susceptibility of heat treated samples in the presence of sulphuric acid environment is further supported by the Nyquist plots in which the diameter of the impedance spectra for the heat treated samples is lower than the control. The oven quenched sample being worst off.

The study therefore reveals that heat treatment caused deterioration of the electrochemical properties of the Alloys AA3003 in sulphuric acid environment.

REFERENCES

Abdel-Gaber AM, Khamis AE, Abo-Eldahab H, Adeel SH (2008).

Inhibition of Aluminium corrosion in alkaline solution using natural compound. Mater. Chem. Phys. 109, 297

Ambat R, Davenport AJ, Scamans GM, Afseth A (2006). Effects of Iron – containing intermetallic particles on the corrosion behaviour of aluminium. Corros. Sci. 48, 3455.

Balaji GA, Radhakrishnan TK (2006). Estimattion of Microbiologically influenced corrosion of aluminium alloy in natural aqueous environment. Nat.andSCi 4(3) p1.

Birbilis N, Buchheit RG (2005). ElectrochemocalCharacteriistics of intermetallic phases in Aluminium Alloys an Experimental survey and Discussion, J. Electrochem. Soc.152(4), B140-B151.

Buchheit RG (1995). A Compilation of corrosion Potential Reported for intermetallic phases in aluminium alloys, J. Electchem.Soc. 142, 11, 3994-3996.

Buchheit RG, Montez LP, Martinez MA, Michael J, Halva PF (1994). Electrochemical Characteristics of Bulk- Synthesized Al_2CuMg. J. Electrochem. Soc. 146, 4424

Cullity BD (1978). *Element of X-Ray Diffraction*, 2nd Ed. 102, Addison-Wesley Pub. Coy California, USA.

Diaz-Ballote L, Lopez-Sansores JF, Maldondo-Lopez L, Garfias-Mesias LF (2009). Corrosion behaviour of aluminium exposed to a bio-diesel. Electrochem Comm. 11, 41

Dymek S, Dollar M (2003). TEM investigation of age-hardenable Al 2519 alloy subjected to stress corrosion cracking tests. Mater. Chem. Phys. 81, 286.

Emreguil KC, AbbasAksilt A (2000). The behavior of aluminium in alkaline media. Corros.Sci.42, 2051.

Fellener P, Chrenkova- Paucivova M, Mataisovsky K (1981). Electrolytic aluminioun plating in molten salt mixtures based on $AlCl_3$ 1: Influence of the addition of tetramethylammonium Chloride. Surf.Technol. 14, 101-108.

Guillaumin V, Mankowski G (1999). Localized corrosion of 2024 T351 aluminium alloy in chloride media. Corros. Sci. 41, 421

Komisarov V, Talianker V, Cina B (1996). Effect of retrogression and re-aging on the precipitates in an 8090 Al–Li alloy. Mater.Scieng. A221, 113.

Li YJ, Arnberg L (2003). Evolution of eutectic intermetallic particlesin DC-Cast AA3003 alloy during heating and homogenization, Mater. Sci. Eng.A, 347.

Liu Y, Cheng YF (2010). The role of second phase particles in pitting corrosion of Al alloy in NaCl solution, Mat. Corros, 61, 3, 211-217.

Nobe K, Nyung N, Chen L, Sumodjo PTO (1999). A comparative Al and Al- Zn alloys electrodissolution and localized corrosion study of 2024 Al in halide media, Electrochemica.Acta.44, 2751.

Okeoma KB, Owate IO, Oguzie EE, Mejeha IM (2011). Impacts of heat treatment on the electrochemical properties of AA3003 expose to 0.1M hydrochloric acid media. American Journ of Mater. Sci. 1(1) 1-7. DOI: 105923/jmaterials 20110920001.

Park JO, Paik CH, Huang YH, Alkire RC (1999). Influence of Fe-rich intermetallic inclusions on pit initiation on aluminium alloy in aerated NaCl. J. Electrochem. Soc. 146, 517.

Rosliza R, WanNik WB, Senin HB (2008). The effect of inhibitor on the corrosion of aluminium alloys in acidic solution Mater. Chem.Phys. 107, 281

Ruhi G, Modi OP, Jha AK, Singh IB (2009). Characterization of corrosion resistance properties of sol-gel aluminium coating in mine water environment. Indian Journ. Chem. Techn. Vol. 16, 216-220.

Santos ML, Acciari HA. Vercik L, Guastaldi LCO (2003). A.C. Effects of 1,4-naphthoquuinone on aluminium corrosion in 0.5 M sodium chloride solution. Mater, Lett. 54, 1888.

Sherif EM, Su-Moon P (2006). Effects of 1,4-naphthoquuinone on aluminium corrosion in 0.5 M sodium chloride solution. ElectrochimicaActa 51, 1313.

Sinyavskii VS (2001). Pitting and stress corrosions of aluminium alloys: correlation between them. Prot. Met.37, 5, 469, DOI: 10.1023/A: 1012374432246.

Stefano C, Alessio F, Alessando L, Ilaria P, Alexander T, Ugo B (2008). Aluminium Electroplated from ionic liquids as protective coating against steel corrosion. Corros.SCi., 50, 534.

Szklarska- Smialowska Z (1999). Pitting Corrosion of Aluminium, Corros.Sce., 41, 1743-1767.

Vargel C (2004). *Corrosion of aluminium,* 100-106, Elssevier, USA, UK

Yang CC (1994). Electrodeposition of aluminum on the high temperature aluminium chloride molten salt systems. Mater.Chem. Phys. 37, 355.